

## Lateral field excitation of thickness shear mode waves in a thin film ZnO solidly mounted resonator

Christopher D. Corso, Anthony Dickherber, and William D. Hunt

Citation: *J. Appl. Phys.* **101**, 054514 (2007); doi: 10.1063/1.2562040

View online: <http://dx.doi.org/10.1063/1.2562040>

View Table of Contents: <http://jap.aip.org/resource/1/JAPIAU/v101/i5>

Published by the [American Institute of Physics](#).

---

### Related Articles

Three-dimensional micro electromechanical system piezoelectric ultrasound transducer  
*Appl. Phys. Lett.* **101**, 253101 (2012)

High energy-storage performance in  $\text{Pb}_{0.91}\text{La}_{0.09}(\text{Ti}_{0.65}\text{Zr}_{0.35})\text{O}_3$  relaxor ferroelectric thin films  
*J. Appl. Phys.* **112**, 114111 (2012)

Intrinsically tunable  $0.67\text{BiFeO}_3\text{-}0.33\text{BaTiO}_3$  thin film bulk acoustic wave resonators  
*Appl. Phys. Lett.* **101**, 232903 (2012)

Nonlinear output properties of cantilever driving low frequency piezoelectric energy harvester  
*Appl. Phys. Lett.* **101**, 223503 (2012)

A review on frequency tuning methods for piezoelectric energy harvesting systems  
*J. Renewable Sustainable Energy* **4**, 062703 (2012)

---

### Additional information on J. Appl. Phys.

Journal Homepage: <http://jap.aip.org/>

Journal Information: [http://jap.aip.org/about/about\\_the\\_journal](http://jap.aip.org/about/about_the_journal)

Top downloads: [http://jap.aip.org/features/most\\_downloaded](http://jap.aip.org/features/most_downloaded)

Information for Authors: <http://jap.aip.org/authors>

## ADVERTISEMENT



**AIP Advances**

Now Indexed in Thomson Reuters Databases

Explore AIP's open access journal:

- Rapid publication
- Article-level metrics
- Post-publication rating and commenting

# Lateral field excitation of thickness shear mode waves in a thin film ZnO solidly mounted resonator

Christopher D. Corso

*School of Biomedical Engineering, Georgia Institute of Technology, Atlanta, Georgia 30332*

Anthony Dickherber and William D. Hunt<sup>a)</sup>

*School of Electrical and Computer Engineering, Georgia Institute of Technology, Atlanta, Georgia 30332*

(Received 7 November 2006; accepted 2 January 2007; published online 14 March 2007)

In recent years, interest in the development of highly sensitive acoustic wave devices as biosensor platforms has grown. A considerable amount of research has been conducted on AT-cut quartz resonators both in thickness excitation and in lateral excitation configurations. In this report, we demonstrate the fabrication of a ZnO solidly mounted resonator operated in thickness shear mode (TSM) using lateral field excitation of the piezoelectric film. Theoretical Christoffel equation calculations are provided to explore the conditions for excitation of a TSM wave in *c*-axis-oriented ZnO through lateral excitation. The existence of a TSM wave is verified through the comparison of theoretical and experimentally obtained acoustic velocity values from frequency versus thickness measurements and water loading of the resonators. A major strength of this design is that it incorporates a simple eight-layer, single-mask fabrication process compatible with existing integrated circuit fabrication processes and can be easily incorporated into multidevice arrays. With minimal electrode optimization, we have been able to fabricate resonators with nearly 100% yield that demonstrate  $Q$  values of up to 550 and  $K^2$  values of 0.88% from testing of more than 30 devices. © 2007 American Institute of Physics. [DOI: 10.1063/1.2562040]

## I. INTRODUCTION AND BACKGROUND

The interest in developing highly sensitive acoustic wave devices for chemical and biological sensing purposes has dramatically increased in the past decade. Acoustic devices offer an attractive alternative to other sensor schemes such as surface plasmon resonance<sup>1</sup> (SPR) and electrochemical sensors<sup>2</sup> because they are small, relatively inexpensive to produce, and offer a potentially superior sensitivity to surface perturbations. The acoustic wave resonating in the piezoelectric cavity acts as a probe querying the surface for any changes in boundary conditions such as mass loading. This is the fundamental concept behind the operation of acoustic biosensors.

In the past, piezoelectric ZnO thin films have been used in the fabrication of thin film bulk acoustic resonators (FBARs) for high frequency filters.<sup>3</sup> Typically, these devices are operated in the thickness-excited longitudinal mode in which the frequency can be tuned simply by varying the thickness of the ZnO thin film. The particle displacement of the propagating acoustic wave in a longitudinal bulk mode is normal to the surface of the film and generates compressional waves in the medium adjacent to the device surface. When operated in an adjacent liquid medium, the longitudinal mode energy is dissipated into the liquid for devices utilizing waves that propagate at a velocity higher than the sound velocity in the liquid. This results in a highly reduced quality factor,  $Q$ , and poor mass resolution in a sensor application. The thickness shear mode (TSM) is better suited for

liquid sensing applications due to the shear particle displacement of the acoustic wave in the piezoelectric film. Since the adjacent liquid medium cannot effectively support a shear wave, very little energy is transferred into the liquid, and this results in minimal damping of the thickness shear mode.

The most common type of TSM resonator is the quartz crystal microbalance (QCM). QCMs are made from thin plates of AT-cut quartz. These devices have been shown to be highly sensitive as gravimetric sensors in both vapor phase and in liquid phase sensing.<sup>4-7</sup> The frequency dependence of the resonator-based biosensor has been characterized by many, including Sauerbrey,<sup>8</sup> Kanazawa and Gordon,<sup>9</sup> and most recently Hunt *et al.*,<sup>10</sup> but all agree that the frequency sensitivity of these devices is proportional to a power of the fundamental resonant frequency  $f_0$ . QCMs typically operate in the frequency range of 5–35 MHz. In AT-cut quartz plates, it is difficult to further increase the fundamental operating frequency because of its dependence on the thickness of the quartz plate. At very low thicknesses, the quartz plate becomes extremely fragile and is difficult to handle. It is possible to achieve higher frequencies with the QCM by monitoring harmonic modes beyond the fundamental, but these become progressively diminished with increasing harmonic number. Solidly mounted FBARs, on the other hand, do not suffer from this problem because the piezoelectric film is grown directly onto a solid foundation. Solidly mounted resonators (SMRs) are made possible by the fabrication of an acoustic mirror directly below the piezoelectric thin film. This so-called Bragg reflector in effect presents the lower side of the piezoelectric material with an acoustic impedance close to that of air over a fairly broad range of frequencies,<sup>11</sup> resulting in the reflection of the acoustic en-

<sup>a)</sup> Author to whom correspondence should be addressed; electronic mail: bill.hunt@ece.gatech.edu

ergy back into the piezoelectric film. This allows for the utilization of extremely thin piezoelectric sensing layers and, ultimately, very high frequency devices (i.e., gigahertz range) can be produced.

The sensitivity of acoustic waves in AT-cut quartz plates has been widely exploited in QCMs which use thickness excitation (TE) to excite the wave. It has been shown, however, that lateral field excitation (LFE) can be used to excite the TSM wave<sup>12–15</sup> and that the resulting device may be more sensitive to surface perturbations than the standard TE QCM for liquid phase sensing applications.<sup>16–19</sup> The advantages of LFE over TE are mainly attributed to the fact that in LFE, the electrodes that generate the electric field are not directly in the path of the acoustic wave, as in TE. Since the metal material that forms the electrode is a source of acoustic wave scattering and damping, its removal from the acoustic path results in higher  $Q$  values. Other advantages include increased stability at a given harmonic and reduced aging of the crystal since the electrode is absent from the area of greatest vibrational motion.<sup>20</sup> For biosensor applications, removing the electrode from the acoustic path means that biological molecules can be immobilized directly onto the region of highest particle displacement which should result in greater sensitivity of the sensor.

There has been varied interest, thus far, in generating a thickness shear mode in ZnO for acoustic devices. One of the more highly investigated methods involves the growth of inclined  $c$ -axis oriented films<sup>21</sup> coupled with an electrode pattern in which the electrodes are situated on opposite sides of the thin film to produce an electric field through the thickness. Wang and Lakin had excellent success in fabricating oriented films with the  $c$ -axis-oriented  $40^\circ$  to the substrate normal.<sup>22</sup> While their resonator  $Q$  and electromechanical coupling were high, the operating frequency was low ( $\sim 293$  MHz) and the fabrication procedure required bulk etching of the Si wafer to produce the air-backed ZnO membrane resonators. More recently, Link *et al.*<sup>23,24</sup> have revived the inclined ZnO growth research with the intent of developing ZnO TSM resonators for liquid phase sensing. A shortcoming of the inclined ZnO growth method is that the thickness excitation requires that the electrodes be in the path of the acoustic wave. While it offers the benefit of a higher operating frequency than the QCM for sensing, it still suffers from the same pitfalls as the QCM because the electrodes are located in the area of highest sensitivity.

In a study by Wei *et al.* focusing on noninclined  $c$ -axis-oriented ZnO, the thickness shear mode was excited through lateral field excitation.<sup>25</sup> The devices were solidly mounted resonators fabricated through the use of a self-aligning process that involved ZnO lift-off and a spiral electrode structure spanning 2 mm in diameter. Operating close to 4.1 GHz, the devices illustrated the ability for ZnO FBARs to be operated at high frequencies with relative ease. However, an acoustic mirror was not implemented in the design, and the quality factor  $Q$  of the resonators was very low (roughly 35). Acoustic velocity calculations we made from the numbers given in the study come out to  $\sim 3280$  m/s as compared to a theoretical value of  $\sim 2841$  m/s calculated

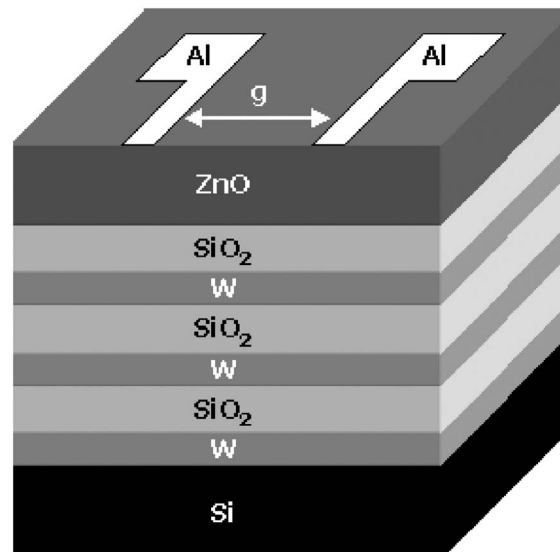


FIG. 1. Electrode and stack configuration.

using bulk stiffness properties of ZnO available in Rosenbaum.<sup>26</sup> This value is reasonable considering variations in ZnO thin film material parameters.

In this paper, we present a laterally excited ZnO thickness shear mode resonator that is both extremely simple to fabricate and highly sensitive to surface perturbations. The resonator configuration consists of a laterally excited, solidly mounted ZnO thin film resonator that incorporates the use of an acoustic mirror. Future investigations will yield optimized electrode designs and even higher performance devices. It should be noted that this device approach is amenable to array format such that multiple target molecules can be simultaneously detected while also providing reference sensors to add statistical significance to the test results. An additional benefit of these devices is the ease of fabrication of repeatable highly  $c$ -axis-oriented ZnO thin films by rf sputtering. We will present data on devices which have been fabricated with a single mask step.

## II. DEVICE FABRICATION AND EXPERIMENTAL PROTOCOL

The overall device design can be seen in Fig. 1. The thin film six-layer stack of alternating W and SiO<sub>2</sub> was deposited by rf magnetron sputtering using the Unifilm PVD-300 sputtering system to create an acoustic reflector analogous to that of a reflector grating in a surface acoustic wave device.<sup>27,28</sup> Scanning electron microscopy (SEM) analysis of the deposition layers demonstrated that we could achieve greater than 90% uniformity of deposition thickness across a 3 in. wafer. The acoustic mirror is designed according to the model described by Lakin.<sup>28</sup> For the desired resonance frequency of approximately 2 GHz, W and SiO<sub>2</sub> thicknesses of 600 and 1200 nm, respectively, were calculated to achieve the desired mirror response. The results of a model simulation based on actual thickness measurements of the fabricated device are shown in Fig. 2. The plot illustrates that over the frequency range of 1.8–2.3 GHz, the reflection coefficient approaches unity. The layers comprising the reflector stack were alternat-

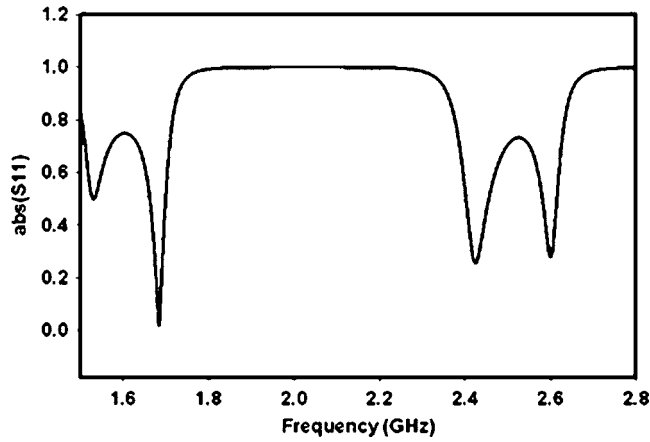


FIG. 2. Simulated reflection coefficient of the acoustic mirror.

ing fused  $\text{SiO}_2$  and W, in which W was the first layer deposited onto a Si (1 0 0) wafer. All sputtering parameters used for the fabrication of these devices are provided in Table I. Following deposition of the stack, a ZnO thin film was sputtered using the Unifilm PVD-300 sputtering system. The final thicknesses of the thin film layers were verified by imaging a cross section of the fabricated wafer using a LEO 1530 thermally assisted field emission (TFE) scanning electron microscope (SEM), and can be seen in Fig. 3. To finish the fabrication procedure, approximately 120 nm of Al was deposited on top of a 30 nm seeding layer of Cr to create the electrodes using a CVC e-beam evaporator and a standard photolithography lift-off process. The electrodes were designed such that the electric field created upon excitation would be perpendicular to the wafer surface normal. This laterally oriented electric field is important for excitation of a bulk acoustic shear wave in the ZnO. To verify the orientation of the electric field resulting from the electrode geometry, electric field simulations were carried out using the COMSOL MULTIPHYSICS<sup>TM</sup> finite element modeling software package. The resonator scattering parameters of the finished devices were obtained using a Cascade Microtech 9000 probe station with Cascade Microtech ACP40-GS/SG probes and analyzed using a HP 8753C network analyzer equipped with a 85047A S parameter test set.

The x-ray diffraction (XRD) data were taken on a Philips X'Pert Materials Research Diffractometer<sup>TM</sup> using a hybrid mirror/monochromator incident optics and a 1/4-degree receiving slit in the diffracted optics beam path. A  $2\theta$ - $\Omega$  rocking-curve scan of the film indicated a strong peak at approximately  $34.26^\circ$ , indicating a (0 0 2) ZnO hexagonal

TABLE I. Sputtering parameters for respective layers using a Unifilm PVD-300 sputterer.

	W	$\text{SiO}_2$	ZnO
Power (W)	0.86 dc	281 rf	142 rf
$\text{O}_2$	NA	2.5%	3%
Ar	100%	97.5%	97%
Temperature ( $^\circ\text{C}$ )	Not heated	Not heated	325
Deposition time (min)	84	139	115
Pressure (torr)	$5.00 \times 10^{-3}$	$5.02 \times 10^{-3}$	$5.10 \times 10^{-3}$

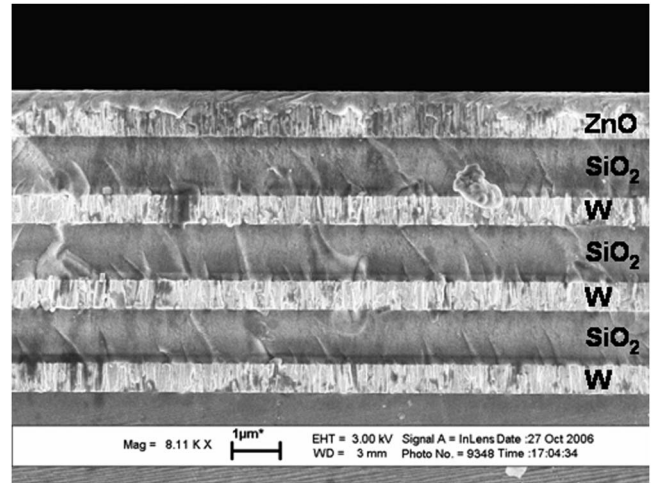


FIG. 3. SEM image of the acoustic mirror and ZnO thin films on a Si substrate.

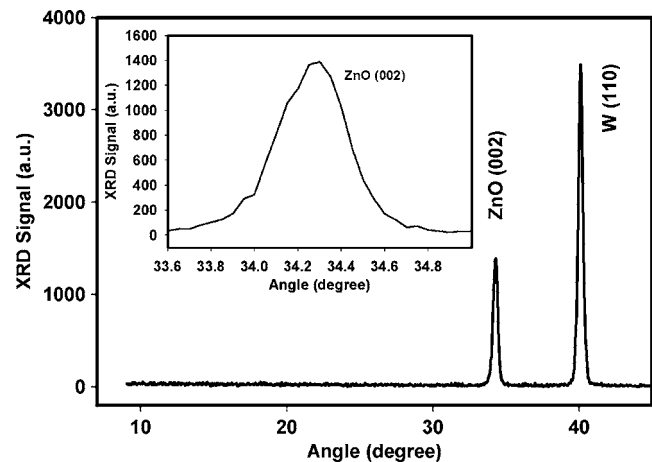
crystal orientation shown in Fig. 4. The peak has a full width at half maximum (FWHM) of  $0.35^\circ$ , indicating a highly oriented  $c$ -axis crystal film. Figure 4 also shows a tight peak at  $40.1^\circ$ , which corresponds to the (1 1 0) orientation of the tungsten layers in the acoustic stack. As expected, no peaks were observed for the  $\text{SiO}_2$  layers in the stack because they are amorphous.

### III. THEORETICAL BACKGROUND AND FINITE ELEMENT MODELING

With the verification of the ZnO crystal orientation in hand, it is possible to solve the Christoffel equation to find the modes of propagation in the bulk given a defined electrical excitation direction. We begin by considering the nonpiezoelectric Christoffel equation

$$(k^2 l_{iK} c_{KL} l_{Lj}) v_j = \rho \omega^2 v_i, \quad (1)$$

where  $k = \tilde{\omega}/v_a$ ,  $\rho$  is the density of the material,  $v_i$  and  $v_j$  are the particle polarization direction vectors, and the  $l_{iK}$  matrix is in the form of

FIG. 4.  $2\theta$ - $\omega$  rocking-curve scan of the ZnO film sputtered on the six-layer W/ $\text{SiO}_2$  acoustic mirror. The inset is a zoomed image of the ZnO peak.

$$l_{iK} = \begin{bmatrix} l_x & 0 & 0 & 0 & l_z & l_y \\ 0 & l_y & 0 & l_z & 0 & l_x \\ 0 & 0 & l_z & l_y & l_x & 0 \end{bmatrix}, \quad (2)$$

where the nonzero terms come from the propagation vector  $\hat{\mathbf{l}} = l_x \hat{\mathbf{i}} + l_y \hat{\mathbf{j}} + l_z \hat{\mathbf{k}}$ . The  $l_{Lj}$  matrix is simply the transpose of  $l_{iK}$ , and  $c_{KL}$  is the material stiffness tensor rotated according to the desired Euler angles. It follows from the XRD data that the ZnO thin films belong to a hexagonal system with a crystal class of 6 mm.

Since the  $c$  axis is oriented normal to the surface, we will arbitrarily choose to align the  $z$  coordinate axis along this crystal axis for our calculations. For thickness shear mode propagation, wave propagation is defined to be in the  $z$  direction, so  $l_x$  and  $l_y$  go to zero and  $l_z$  goes to 1.

Equation (1) is used to solve for directions and velocities of bulk waves propagating in the substrate, but it does not account for the piezoelectric properties of a material nor the possibility of the generation of these waves by an electric field. For this reason, we turn to the piezoelectric Christoffel equation

$$k^2 \left\{ l_{iK} \left[ c_{KL}^E + \frac{(e_{Kj} m_j)(m_i e_{iL})}{m_i \varepsilon_{ij}^S m_j} \right] l_{Lj} \right\} v_j = \rho \omega^2 v_i, \quad (3)$$

where  $e_{Kj}$  is the piezoelectric coupling tensor,  $\varepsilon_{ij}^S$  is the  $3 \times 3$  permittivity tensor at constant strain,  $m$  is the vector corresponding to the direction of the electric excitation field, and now  $c_{KL}^E$  corresponds to the  $6 \times 6$  stiffness tensor at a constant electric field. As can be seen, Eq. (3) is similar to Eq. (1) but for the inclusion of the piezoelectric and permittivity tensors, which apply piezoelectric “stiffening” to the stiffness tensor.

For the lateral field excitation of the  $c$ -axis-oriented ZnO, we desire the electric excitation field to be orthogonal to the wave propagation. Therefore, if the wave propagation is in the direction of the  $z$  axis, the electric field is in the  $x$ - $y$  plane. Here, we will describe the coupling and acoustic wave propagation for the general case of an electric field along any direction within the  $x$ - $y$  plane. The electric field vector  $m_j$  is of the form

$$m_j = \begin{bmatrix} m_x \\ m_y \\ m_z \end{bmatrix}. \quad (4)$$

Solving the piezoelectrically stiffened Christoffel equation for laterally excited ZnO, we set  $m_z=0$  and  $m_x^2+m_y^2=1$ . The 6 mm hexagonal system stiffness tensor is of the form

$$c = \begin{bmatrix} c_{11} & c_{12} & c_{13} & 0 & 0 & 0 \\ c_{12} & c_{11} & c_{13} & 0 & 0 & 0 \\ c_{13} & c_{13} & c_{33} & 0 & 0 & 0 \\ 0 & 0 & 0 & c_{44} & 0 & 0 \\ 0 & 0 & 0 & 0 & c_{44} & 0 \\ 0 & 0 & 0 & 0 & 0 & c_{66} \end{bmatrix}, \quad (5)$$

and the form of the piezoelectric matrix is

$$e = \begin{bmatrix} 0 & 0 & 0 & 0 & e_{15} & 0 \\ 0 & 0 & 0 & e_{15} & 0 & 0 \\ e_{31} & e_{31} & e_{33} & 0 & 0 & 0 \end{bmatrix}. \quad (6)$$

The resulting Christoffel matrix is of the form

$$\Gamma = \begin{bmatrix} c_{44} + e_{15}^2 m_x^2 / \varepsilon_{11} & e_{15}^2 m_x m_y / \varepsilon_{11} & 0 \\ e_{15}^2 m_x m_y / \varepsilon_{11} & c_{44} + e_{15}^2 m_y^2 / \varepsilon_{11} & 0 \\ 0 & 0 & c_{33} \end{bmatrix}. \quad (7)$$

The eigenvalues of this matrix correspond to terms that can be used to solve for  $v_a$ , the acoustic velocity in each of the three wave propagation modes, while the corresponding eigenvectors relate to the direction of particle displacement. Solving for the eigenvectors and eigenvalues of  $\Gamma$  gives

$$x_1 = \begin{bmatrix} -m_y \\ m_x \\ 0 \end{bmatrix}, \quad \lambda_1 = c_{44}; \quad x_2 = \begin{bmatrix} m_x \\ m_y \\ 0 \end{bmatrix}, \quad (8)$$

$$\lambda_2 = c_{44} + \frac{e_{15}^2}{\varepsilon_{11}}; \quad x_3 = \begin{bmatrix} 0 \\ 0 \\ 0 \end{bmatrix}, \quad \lambda_3 = c_{33}.$$

From these results, we find that only one mode is piezoelectrically excited (defined by  $x_2$  and  $\lambda_2$ ) and that the particle displacement will be directly aligned with the electric field, regardless of the orientation of the field with respect to the  $x$ - $y$  plane. This mode is a pure shear thickness mode and is the mode we seek. Another pure shear mode exists (defined by  $x_1$  and  $\lambda_1$ ) with particle displacement also in the  $x$ - $y$  plane at an angle perpendicular to that of the piezoelectrically excited mode; however, it is piezoelectrically inactive. The longitudinal mode (defined by  $x_3$  and  $\lambda_3$ ), importantly, is also piezoelectrically inactive. These results indicate that an electric field in the  $x$ - $y$  plane will excite a pure shear thickness mode with particle displacement aligned with the electric field. The acoustic velocity for this mode can be calculated from

$$v_a = \sqrt{\frac{c_{44} + e_{15}^2 / \varepsilon_{11}}{\rho}}. \quad (9)$$

Using bulk values for ZnO from Rosenbaum,<sup>26</sup>  $e_{15} = -0.48$ ,  $c_{44} = 43 \times 10^9$  N/m<sup>2</sup>,  $\varepsilon_{11} = 8.6$  (rel.), and  $\rho = 5700$  kg/m<sup>3</sup>, the theoretical acoustic velocity for the piezoelectrically stiffened thickness shear mode is approximately 2841 m/s. Since most ZnO thin films include various dopants and are not of pure crystal uniformity, they will have stiffness, density, and piezoelectric constants that are different from these bulk values. This calculated acoustic velocity is therefore an approximate figure and not an absolute value from which to evaluate an experimentally obtained mode. The theoretical piezoelectric coupling constant for the ZnO LFE resonator is given by

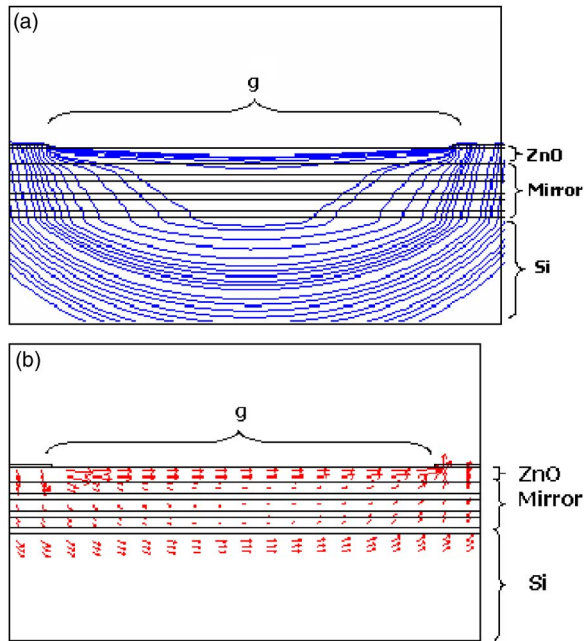


FIG. 5. (Color online) Finite element simulation plots illustrating the electric field characteristics resulting from the electrode configuration in Fig. 1. (a) shows the electric field streamline plot and (b) shows an arrow plot where the electric field direction is indicated by the direction of the arrow, and the relative strength of the electric field (C/m) is indicated by the size of the arrow.

$$K^2 = \frac{e_{15}^2}{c_{44}\epsilon_{11}}, \quad (10)$$

which is calculated to be approximately 0.07 or 7% for the case of the thickness shear mode.

All of the above calculations rely on the assumption that the lateral excitation field is aligned in the  $x$ - $y$  plane. Therefore, it is important to verify that a given electrode structure generates an electric field consisting of a primarily lateral component. To accomplish this, the electromagnetics module of the COMSOL MULTIPHYSICS® finite element modeling software package was used to evaluate the electrode configuration. While multiple electrode geometries have been investigated, only the most basic structure, as shown in Fig. 1, will be discussed here for the sake of simplicity.

Figure 5(a) shows a streamline plot of the electric field lines produced from the simple electrode geometry with a gap of 20  $\mu\text{m}$ . The streamlines visualize the direction of the electric field lines with no information about the strength of the vector field. Figure 5(b) is an image of the electric field produced by the gap depicted through arrows which illustrate the direction (orientation of arrow) and relative intensity of the electric field (size of arrow) in the ZnO. The plots specify that the electric field is aligned parallel to the surface in the area between the gaps, while it is aligned primarily normal to the surface in the area directly below the electrodes. The relative sizes of the arrows in Fig. 5(b) show that the relative strength of the electric field within the electrode gap is approximately twice that of the electric field directly beneath the electrodes (data not shown). These plots indicate that the electric field generated by the proposed electrode configuration will generate a laterally oriented field in the active area

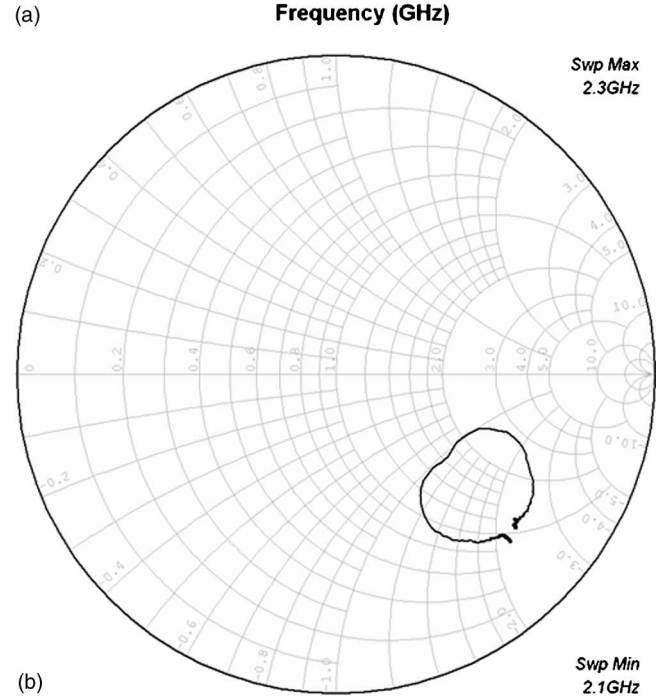
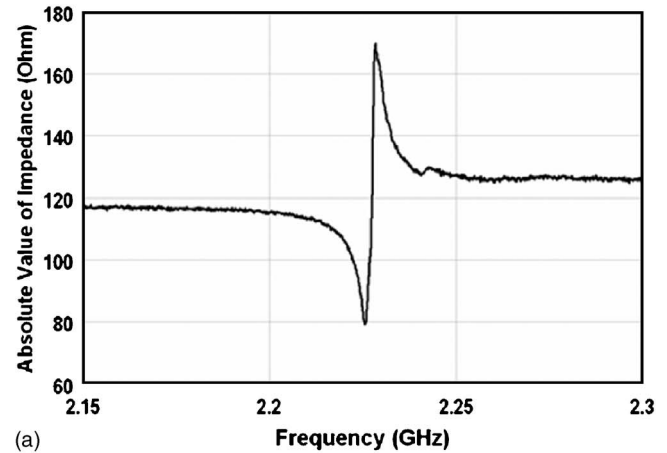


FIG. 6. Network analyzer probe measurements showing (a) the magnitude of the impedance response as a function of frequency and (b) the  $S_{11}$  Smith chart plot.

of the device with a minimal surface-normal component which is a requisite for lateral field excitation. Further, it is indicated that a weak response due to thickness excitation of the longitudinal mode is expected.

#### IV. RESULTS AND DISCUSSION

RF probing of individual devices yielded thickness shear mode activity in the ZnO devices over a range of ZnO thin film thicknesses. Testing the acoustic response by fabricating wafers with multiple thicknesses of ZnO is important for verifying that the  $S_{11}$  response is due to an acoustic phenomenon rather than some electromagnetic resonance. This can be done by verifying that as the film thickness changes, the resonant frequency changes accordingly. Probing of more than 30 devices yielded impedance and  $S_{11}$  responses similar to those shown in Fig. 6. As can be seen from the Smith chart [Fig. 6(b)], a clear loop pattern, indicative of resonant activity, is present. An average unloaded  $Q$  of these resonators is

TABLE II. Result of changing ZnO thickness on resonator response.

Measured ZnO thickness (nm)	$f_0$ (GHz)	Extracted acoustic velocity (m/s)
790	2.0	3160
710	2.2	3130
660	2.35	3100

approximately 340 and the  $K^2$  is approximately 0.4%, with peak values of 550 and 0.88%, respectively. The calculations used to assess  $Q$  and  $K^2$  are<sup>26,28</sup>

$$Q = \left(\frac{f}{2}\right) \frac{d \angle Z}{df}, \quad (11)$$

$$K^2 = \left(\frac{\pi}{2}\right)^2 \frac{f_p - f_s}{f_p}. \quad (12)$$

The acoustic velocity was empirically determined to be on the average of 3130 m/s. This is somewhat close to the theoretical value of 2841 m/s, but much closer to the experimental value of 3280 m/s, as calculated from the results of Woo Wai *et al.*<sup>29</sup> The theoretical longitudinal velocity for ZnO is approximately 6300 m/s. This value is much higher than the experimentally obtained acoustic velocity, and is therefore a good indicator that it is the shear mode that is being excited and not the longitudinal. Interestingly, no longitudinal peak was found to exist throughout the frequency spectrum of the resonators and may be attributed to poor reflection characteristics of the mirror at the longitudinal frequency. This can also be explained by the weak electric field component normal to the surface generated by the electrode configuration. To further confirm acoustic wave resonance, we altered the thickness of the ZnO to demonstrate that increasing the film thickness resulted in a corresponding decrease in resonant frequency. The results of these tests are summarized in Table II. We feel that the resonance could be significantly improved through optimization of the electrode configuration to enhance piezoelectric coupling of the electric field energy to the crystal and to provide energy trapping for the acoustic wave.

Aside from comparing the experimentally obtained acoustic velocity to the TSM and longitudinal velocities, another way to further establish the existence of a thickness shear mode is to expose the resonators to water at the surface. If the acoustic activity were longitudinal, application of de-ionized water at the surface would decimate the acoustic resonance observed in the device since water can support a longitudinal wave, but not a shear wave. Figure 7 shows the response before (triangles) and after (squares) application of de-ionized water to the surface. As can be seen, the water had only small effects on the suppression seen in the  $S_{11}$  magnitude response, and a negative frequency shift occurred after water was applied to the device of approximately 1.1 MHz. According to Sauerbrey,<sup>8</sup> this response is to be expected from a TSM device, roughly described in his equation

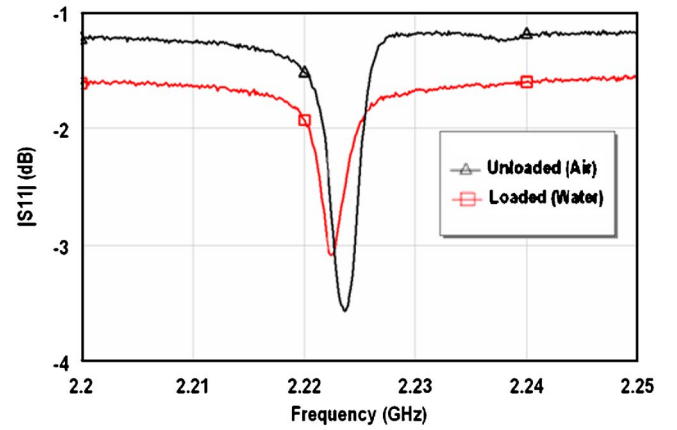


FIG. 7. (Color online) Frequency shift observed in  $S_{11}$  measurement in response to loading the surface of the resonator with de-ionized  $H_2O$ . Some deterioration of the resonance was observed resulting in the decrease of the  $Q$  factor.

$$\Delta f = \left(\frac{-2f_0^2}{A\sqrt{\rho_q\mu_q}}\right) \Delta m_q, \quad (13)$$

where  $f_0$  is the resonant frequency of the device,  $A$  is the relevant area,  $\rho_q$  is the material density,  $\mu_q$  is the material stiffness, and  $\Delta m_q$  is the change in mass at the surface. It is reasonable to assume that the observed frequency shift indicates a mass loading on the surface of the device by the de-ionized water. This would also confirm the prediction made by analysis of the Christoffel matrix that the wave is a TSM wave. The response to the water test was shown to be repeatable across different devices in various locations about the wafer.

## V. CONCLUSIONS

Theoretical analysis of the Christoffel equation has shown that a TSM wave can be excited in  $c$ -axis-oriented ZnO with an in-plane excitation field oriented in any direction on the wafer. Further, it has been shown that the shear particle displacement will be parallel to the excitation field, assuming an entirely lateral field.

To implement the theoretical findings, a solidly mounted resonator consisting of alternating layers of W and  $SiO_2$  were grown on a  $p$ -doped  $\langle 1\ 0\ 0 \rangle$  Si substrate with ZnO as the active piezoelectric layer at the surface. The acoustic mirror was designed to have a reflection coefficient closest to unity near the frequency of operation. The acoustic mirror frequency response was simulated to provide assurance of the frequency range coverage given a fixed number of alternating pairs of W and  $SiO_2$ . Finite element modeling was also performed to predict the electric field of an electrode configuration consisting of two long electrodes positioned on the top of the ZnO with a gap between them. Simulations showed that the electric field within the gap between the electrodes was primarily laterally oriented, while the electric field directly beneath the electrodes was shown to be reduced in magnitude with an orientation normal to the surface of ZnO.

To verify the thickness shear mode operation of the devices, we investigated the experimentally extracted acoustic

velocity and the effects of water loading on the resonance. Without these tests it is difficult to adequately determine that a resonance is necessarily TSM. We have presented evidence of a TSM wave through exposure of the device to de-ionized water, comparison of extracted acoustic velocity with theoretical acoustic velocity, and varying the piezoelectric film thickness to yield respective changes in the frequency response.

On the basis of these results, it is expected that with an appropriate chemical surface preparation, these devices could be used as a platform for biosensor applications. The simple fabrication and small device size make this an appropriate candidate for fabrication of sensor arrays. The results of our investigation indicate that the lateral excitation of a thickness shear mode in solidly mounted ZnO FBARs is realizable both theoretically and experimentally. In the future, we will experiment with multiple electrode geometries in order to improve device response and performance.

## ACKNOWLEDGMENTS

This work was supported by the Georgia Tech/Emory Fund for Innovative Cancer Technologies which derives its funds from The V Foundation and the Georgia Cancer Coalition. In addition, Chris Corso was supported by a NSF Graduate Research Fellowship. Further, we must acknowledge the support of Dr. Colin Wood of the Office of Naval Research under the MURI program "Epitaxial Multifunctional Materials and Applications." We would also like to thank John Perng and Brent Buchine for their time and help with obtaining the SEM images. The support of all of these organizations is very much appreciated.

<sup>1</sup>J. W. Chung, J. M. Park, R. Bernhardt, and J. C. Pyun, *J. Biotechnol.* (2006).

<sup>2</sup>M. S. Wilson and W. Nie, *Anal. Chem.* **78**, 6476 (2006).

<sup>3</sup>S. L. Pinkett, W. D. Hunt, B. P. Barber, and P. L. Gammel, *IEEE Trans. Ultrason. Ferroelectr. Freq. Control* **49**, 1491 (2002).

<sup>4</sup>A. Shons, F. Dorman, and J. Najarian, *J. Biomed. Mater. Res.* **6**, 565 (1972).

<sup>5</sup>X. L. Su and Y. Li, *Biosens. Bioelectron.* **19**, 563 (2004).

<sup>6</sup>Z. Y. Wu, G. L. Shen, S. P. Wang, and R. Q. Yu, *Anal. Sci.* **19**, 437 (2003).

<sup>7</sup>C. D. Corso, D. D. Stubbs, S. H. Lee, M. Goggins, R. H. Hruban, and W. D. Hunt, *Cancer Detect. Prev.* **30**, 180 (2006).

<sup>8</sup>G. Sauerbrey, *Z. Phys.* **155**, 206 (1959).

<sup>9</sup>K. K. Kanazawa and J. G. Gordon, *Anal. Chem.* **57**, 1770 (1985).

<sup>10</sup>W. D. Hunt, D. D. Stubbs, and L. Sang-Hun, *Proc. IEEE* **91**, 890 (2003).

<sup>11</sup>S. L. Pinkett, Ph.D. thesis, Georgia Institute of Technology, 2003.

<sup>12</sup>J. V. Atanasoff and P. J. Hart, *Phys. Rev.* **59**, 85 (1941).

<sup>13</sup>R. Bechmann, 14th Annual Symposium on Frequency Control (US Army Electronics Research and Development Laboratory, Atlantic City, NJ, 1960), pp. 68–88.

<sup>14</sup>E. R. Hatch and A. Ballato, *Ultrason. Symp. Proc. (IEEE Group on Sonics & Ultrasonics, Atlanta, GA, 1983)*, p. 512

<sup>15</sup>A. W. Warner, 17th Annual Symposium on Frequency Control (US Army Electronics Research and Development Laboratory, Atlantic City, NJ, 1963), pp. 248–266.

<sup>16</sup>H. Yihe, L. A. French, Jr., K. Radecsky, M. Pereira da Cunha, P. Millard, and J. F. Vetelino, *IEEE Trans. Ultrason. Ferroelectr. Freq. Control* **51**, 1373 (2004).

<sup>17</sup>H. Yihe, L. A. French, Jr., K. Radecsky, M. Pereira da Cunha, P. Millard, and J. F. Vetelino *IEEE Trans. Ultrason. Ferroelectr. Freq. Control* **51**, 1373 (2004).

<sup>18</sup>W. Pinkham, M. Wark, S. Winters, L. French, D. J. Frankel, and J. F. Vetelino, *Proc.-IEEE Ultrason. Symp.* **4**, 2279 (2005).

<sup>19</sup>C. York, L. A. French, P. Millard, and J. F. Vetelino, *Proc.-IEEE Ultrason. Symp.* **1**, 44 (2005).

<sup>20</sup>A. Ballato, E. R. Hatch, M. Mizan, and T. J. Lukaszczek, *IEEE Trans. Ultrason. Ferroelectr. Freq. Control* **33**, 385 (1986).

<sup>21</sup>S. V. Krishnaswamy, B. R. McAvoy, W. J. Takei, and R. A. Moore, *Ultrason. Symp. Proc. (IEEE Group on Sonics & Ultrasonics, San Diego, CA, 1982)*, p. 476.

<sup>22</sup>J. S. Wang and K. M. Lakin, *Ultrason. Symp. Proc. (IEEE Group on Sonics & Ultrasonics, San Diego, CA, 1982)*, p. 480.

<sup>23</sup>M. Link *et al.*, *J. Vac. Sci. Technol. A* **24**, 218 (2006).

<sup>24</sup>M. Link, M. Schreiter, J. Weber, R. Primig, D. Pitzer, and R. Gabl, *IEEE Trans. Ultrason. Ferroelectr. Freq. Control* **53**, 492 (2006).

<sup>25</sup>P. Wei, Y. Hongyu, K. Jae Wan, Z. Hao, and K. Eun Sok, *Proceedings of the 2004 IEEE International Frequency Control Symposium and Exposition*, (IEEE UFFC Society, Montreal, Canada, 2004) pp. 558–561.

<sup>26</sup>J. F. Rosenbaum, *Bulk Acoustic Wave Theory and Devices* (Artech House, Boston, 1988).

<sup>27</sup>W. E. Newell, *Proc. IEEE* **53**, 575 (1965).

<sup>28</sup>K. M. Lakin, G. R. Kline, and K. T. McCarron, *IEEE Trans. Microwave Theory Tech.* **43**, 2933 (1995).

<sup>29</sup>L. Woo Wai, S. Yonghua, and K. Eun Sok, *Proceedings of the 1996 IEEE International Frequency Control Symposium* (IEEE UFFC Society, New Brunswick, NJ, 1996), pp. 558–562.